# Exactly Solvable Fermion Chain Describing a $\nu = 1/3$ Fractional Quantum Hall State

Masaaki Nakamura,[1] Zheng-Yuan Wang,[1] and Emil J. Bergholtz[2]

[1]*Department of Physics, Tokyo Institute of Technology, O-Okayama, Meguro-ku, Tokyo 152-8551, Japan*

[2]*Dahlem Center for Complex Quantum Systems and Institut für Theoretische Physik, Freie Universität Berlin, Arnimallee 14, 14195 Berlin, Germany*

(Received 25 October 2011; published 2 July 2012)

We introduce an exactly solvable fermion chain that describes a $\nu = 1/3$ fractional quantum Hall (FQH) state beyond the thin-torus limit. The ground state of our model is shown to be unique for each center-of-mass sector, and it has a matrix product representation that enables us to exactly calculate order parameters, correlation functions, and entanglement spectra. The ground state of our model shows striking similarities with the BCS wave functions and quantum spin-1 chains. Using the variational method with matrix product ansatz, we analytically calculate excitation gaps and vanishing of the compressibility expected in the FQH state. We also show that the above results can be related to a $\nu = 1/2$ bosonic FQH state.

DOI: 10.1103/PhysRevLett.109.016401 PACS numbers: 71.10.Pm, 73.43.Cd, 75.10.Kt

*Introduction.*—The fractional quantum Hall (FQH) effect is one of the fascinating phenomena in condensed matter physics: In a 2D electron system in a magnetic field, the Hall conductivity is quantized as $\sigma_H = (e^2/h)\nu$ with the filling factor given by a rational number $\nu = p/q$, due to strong electron-electron interactions [1,2]. Although three decades have past since its discovery, the importance of this research field is still increasing, partly due to new possible realizations of FQH phenomena, including flat band Chern insulators [3] and bosonic systems of trapped atoms [4].

In recent years, there have been theoretical efforts to study FQH states in torus boundary conditions which can reduce the 2D continuum system in a magnetic field to a 1D lattice model [5,6]. This approach sheds new light on the FQH physics and is also used to analyze new type of FQH states in flat band Chern insulators [7].

In this Letter, based on the 1D approach, we introduce a minimal model with an exact ground state which describes a $\nu = 1/3$ FQH state [Eq. (3) below]. We construct the Hamiltonian in terms of local positive operators much like the Affleck, Kennedy, Lieb, and Tasaki model for a quantum spin-1 chain [8]. We discuss the properties of this model by obtaining exact expressions for various correlation functions, order parameters, and entanglement spectra. Moreover, excitation gaps are accurately obtained via variational calculations.

*1D description of FQH states.*—We consider 2D interacting electrons in a magnetic field $B$ on toroidal boundary conditions, where $L_i$ $(i = 1, 2)$ are the circumferences of the torus of the corresponding coordinates $x_i$, and $l_B \equiv \sqrt{\hbar/eB}$ is the magnetic length which will be set to unity. As discussed in preceeding works [5,6], the system with two-body interaction assumes the following 1D discretized model,

$$\mathcal{H} = \sum_{i=1}^{N_s} \sum_{k>|m|} V_{km} c_{i+m}^\dagger c_{i+k}^\dagger c_{i+m+k} c_i, \tag{1}$$

where $c_i^\dagger$ $(c_i)$ creates (destroys) a fermion at site $i$, and the number of lattice sites is given by $N_s = L_1 L_2/2\pi$. The matrix-element $V_{km}$ specifies the amplitude for a process where two particles with separation $k + m$ hop $m$ steps to opposite directions. This process conserves the center-of-mass coordinate $K_1 \equiv \sum_{i=1}^{N_s} i\hat{n}_i \pmod{N_s}$ with $\hat{n}_i \equiv c_i^\dagger c_i$, which corresponds to the momentum along $x_1$ direction. Therefore, the system with $\nu = p/q$ can be divided into $q$ independent subsystems.

For the pseudopotential [9] which has the $\nu = 1/3$ Laughlin wave function [2] as an exact ground state, the matrix elements for large $L_2$ are

$$V_{km} \propto (k^2 - m^2) e^{-2\pi^2(k^2+m^2)/L_1^2}. \tag{2}$$

Thus the hopping terms $(m \neq 0)$ are suppressed exponentially compared to the electrostatic terms $(m = 0)$ in the thin-torus (TT) limit $L_1 \to 0$, and the system becomes a charge-density-wave state $\Psi_0 = |100100100\cdots\rangle$. In order to describe systems with finite $L_1$, we include also the leading hopping terms. This expansion in $e^{-2\pi^2/L_1^2}$ is well controlled, and we expect it to capture the physics also for more general interactions [5,6,10–12].

*Model with exact ground state.*—Based on the above framework, we truncate the long-range interactions of the 1D model (1) at $\nu = 1/3$ up to the third neighbor $(k + m \leq 3)$ assuming only $\sqrt{V_{10}V_{30}} = V_{21}$ which is satisfied in Eq. (2), $\forall L_1$. Then we have

$$\mathcal{H} = \sum_{i=1}^{N_s} [\alpha_i^2 \hat{n}_{i+1}\hat{n}_{i+2} + \beta_i^2 \hat{n}_i \hat{n}_{i+2} + \gamma_i^2 \hat{n}_i \hat{n}_{i+3} + \alpha_i \gamma_i (c_i^\dagger c_{i+3}^\dagger c_{i+2} c_{i+1} + \text{H.c.})], \tag{3}$$

where we have generalized the parameters $\alpha_i$, $\beta_i$, $\gamma_i \in \mathbf{R}$ to have site dependence. This truncation is valid as an expansion beyond the TT limit [13]. Now, we rewrite this model in the following form:

 

$$\mathcal{H} = \sum_i [Q_i^\dagger Q_i + P_i^\dagger P_i], \tag{4}$$

where

$$Q_i = \alpha_i c_{i+1} c_{i+2} + \gamma_i c_i c_{i+3}, \qquad P_i = \beta_i c_i c_{i+2}. \tag{5}$$

Equation (4) is clearly a sum of positive operators, thus, the spectrum is positive semidefinite $\langle \mathcal{H} \rangle \geq 0$. As we will show, the (unnormalized) ansatz,

$$|\Psi_{1/3}\rangle = \prod_i (1 - t_i \hat{U}_i)\Psi_0 = \prod_i e^{-t_i \hat{U}_i} |\Psi_0\rangle, \tag{6}$$

where $t_i \equiv \gamma_i/\alpha_i$ and $\hat{U}_i \equiv c_{i+1}^\dagger c_{i+2}^\dagger c_{i+3} c_i$, provides the unique zero energy solutions. Note that $[\hat{U}_i, \hat{U}_j] = 0$ for $|i - j| \neq 2$ and $\hat{U}_i \hat{U}_{i+2} |\Psi_0\rangle = 0$. In Eq. (6), the original state $|\cdots 1001 \cdots\rangle$ in $|\Psi_0\rangle$ and its "squeezed" counterpart $|\cdots 0110 \cdots\rangle$ cancel each other by acting $Q_i$, and there are no next-nearest pairs $|\cdots 101 \cdots\rangle$. Hence, this state satisfies $Q_i |\Psi_{1/3}\rangle = P_i |\Psi_{1/3}\rangle = 0$, $\forall i$, and it is a zero-energy ground state [14]. Due to the conservation of the center of mass, this state has threefold degeneracy for periodic systems, even when the parameters have site dependence. Our wave function (6) gives exact ground states for open boundary systems. We can obtain many new zero-energy eigenstates at a lower filling than $\nu = 1/3$ by inserting an extra 0 anywhere in the root state, $|\Psi_0\rangle$ in (6), because the insertion of 0 is equivalent to make open boundaries. Moreover, if . . .000101 type configurations are located at these "edges", they also give eigenstates with finite energies due to the $\beta_i^2$ term.

The uniqueness of the ground state for each center-of-mass sector in the $\nu = 1/3$ periodic case can be shown using the Perron-Frobenius theorem. First, one can show that all the states generated by acting with the Hamiltonian on $|\Psi_0\rangle$ can be reached by successive applications of $\hat{U}_i$ (for different $i$) [15]; thus, the Hamiltonian takes the form of a connected matrix in this subspace. Next, with a unitary transformation that changes the signs of $\gamma_i$, all the off-diagonal matrix elements can be made negative. Now, the Perron-Frobenius theorem implies that there are no other zero-energy states than (6) in this subspace, since all its expansion coefficients have the same sign. Finally, it follows that all states that are not connected to $|\Psi_0\rangle$ (or translations thereof) by the Hamiltonian always include finite amplitudes of next-nearest neighbor particle which costs energy when $\beta_i^2 > 0$; thus, all such states have a finite energy. This concludes the proof that (6) is the unique ground state up to translations.

*Correlation functions and order parameters.*—From the exact solution (6) it is possible to calculate rather generic quantities such as correlation functions and entanglement properties of the ground state. For this purpose, it is convenient to introduce a matrix product (MP) representation [16,17] of the ground state wave function (6). In a periodic system with $N_s = 3N$ sites, the normalized ground state wave function (6) can be written as

$$|\Psi_{1/3}\rangle = \mathcal{N}^{-1/2} \mathrm{tr}[g_1 g_2 \cdots g_N], \tag{7}$$

where $g_j$ is identified as the following $2 \times 2$ matrix:

$$g_j = \begin{bmatrix} |\mathrm{o}\rangle_j & |+\rangle_j \\ -t_{3j}|-\rangle_j & 0 \end{bmatrix}. \tag{8}$$

Here, we have introduced the spin-1 representation for three-sites unit cell [18]: $|010\rangle \to |\mathrm{o}\rangle$, $|001\rangle \to |+\rangle$, and $|100\rangle \to |-\rangle$. For the open boundary system, we should extract only (1, 1) component of (7) instead of taking the trace.

Using the MP formalism for uniform $t_i = t$ and infinite systems $N \to \infty$, we obtain the density function which has three-site periodicity as [see Fig. 1(a)]

$$\langle \hat{n}_{3i\pm1} \rangle = \frac{1}{2}\left(1 - \frac{1}{\sqrt{4t^2 + 1}}\right), \qquad \langle \hat{n}_{3i} \rangle = \frac{1}{\sqrt{4t^2 + 1}}. \tag{9}$$

This result shows that the density function becomes uniform at $t = \pm\sqrt{2}$ [19]. The single particle correlation function is given by $\langle c_i^\dagger c_j \rangle = \delta_{ij} \langle \hat{n}_i \rangle$ due to the center-of-mass conservation.

We can also obtain density-density correlation functions in a similar way. In the infinite-size limit, we find exponentially decaying correlations

$$\langle n_i n_j \rangle - \langle n_i \rangle \langle n_j \rangle \sim \left(\frac{1 - \sqrt{4t^2 + 1}}{1 + \sqrt{4t^2 + 1}}\right)^{|i-j|/3} \equiv e^{-|i-j|/\xi}. \tag{10}$$

As $|t| \to \infty$, the correlation length $\xi$ diverges which reflects the state $|+-+-\cdots\rangle + |-+-+\cdots\rangle$.

Using the suggestive analogy of quantum spin-1 chains, we consider nonlocal order in terms of the string order

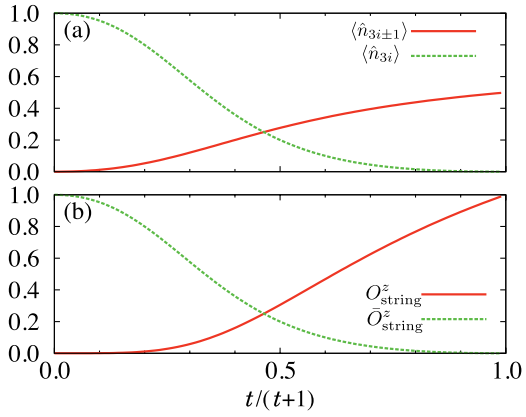


FIG. 1 (color online). (a) Density functions $\langle \hat{n}_i \rangle$ in three-sites unit cell, and (b) String order parameter $O^z_{\mathrm{string}}$ and dual string order parameter $\bar{O}^z_{\mathrm{string}}$ as functions of $t$. $O^z_{\mathrm{string}}$ ($\bar{O}^z_{\mathrm{string}}$) dominant in the large (small) $t$ regime plays a role to characterize the "superconducting" ("normal") component in an analogy of the BCS theory.

parameters $O^{\alpha}_{\rm string} = -\langle S^{\alpha}_i e^{i\pi\sum_{k=i+1}^{j-1} S^{\alpha}_k} S^{\alpha}_j\rangle$ [20]. This is known to characterize the Haldane-gap (including Néel) state. On the other hand, a "dual" string order parameter $\bar{O}^{\alpha}_{\rm string} = \langle e^{i\pi\sum_{k=i+1}^{j-1} S^{\alpha}_k}\rangle$ [21] can be introduced to characterize the large-$D$ phases. Using the MP formalism we find

$$O^{z}_{\rm string} = \frac{(\sqrt{4t^2+1}-1)^2}{4t^2+1}, \qquad \bar{O}^{z}_{\rm string} = \frac{1}{4t^2+1}, \quad (11)$$

where $N$, $j-i \to \infty$ is assumed, and the $x$, $y$ components are vanishing. In conventional quantum spin chains, these two order parameters are usually not finite simultaneously. However, the present spin-mapped system breaks the space-inversion and spin-reversal symmetries (e.g., a configuration $|\cdots + -\mathrm{o}\cdots\rangle$ occur in (7) but $|\cdots \mathrm{o} - +\cdots\rangle$ does not), and also SU(2) symmetry, which enables the two different orders to coexist. This results consistent with the numerical analysis which concludes that the spin-mapped $\nu = 1/3$ FQH state is adiabatically connected both from "Haldane" (Néel) and large-$D$ phases without closing the energy gap [18,21,22]. The two string order parameters behave as $O^{z}_{\rm string} \to 1$ for $|t| \to \infty$ and $\bar{O}^{z}_{\rm string} \to 1$ for $t \to 0$ as shown in Fig. 1(b). This can be interpreted as the two limits characterize "superconducting" and "normal" states in analogy with the BCS wave function which is very similar to Eq. (6)—it has the form of bosonic operators acting on a vacuum state.

*Entanglement spectrum and entropy.*—We can also derive the entanglement spectrum (ES) $\{\xi_i\}$ [23] of the system in the spin-1 MP basis via the Schmidt decomposition dividing the system into two parts, $\{k_1, \ldots, k_L\} \in A$ and $\{k_{L+1}, \ldots, k_N\} \in B$, as

$$\begin{aligned}|\Psi_{1/3}\rangle &= \mathcal{N}^{-1/2} \sum_{j_1,j_2=1,2} \{[g_1 \cdots g_L]_{j_1 j_2} [g_{L+1} \cdots g_N]_{j_2 j_1}\} \\ &= \sum_{j_1,j_2=1,2} (\mathcal{N}^{A}_{j_1,j_2} \mathcal{N}^{B}_{j_1,j_2}/\mathcal{N})^{1/2} |\psi^{A}_{j_1,j_2}\rangle \otimes |\psi^{B}_{j_1,j_2}\rangle \\ &\equiv \sum_i e^{-\xi_i/2} |\psi^{A}_i\rangle \otimes |\psi^{B}_i\rangle, \end{aligned} \quad (12)$$

where $|\psi^{A(B)}_i\rangle$ with $i \equiv (j_1, j_2)$ are orthogonal states describing subsystem $A(B)$, and $\mathcal{N}^{A(B)}_{j_1,j_2}$ are their norms. In the infinite-size limit, $L = N/2 \to \infty$, one finds $\xi_1$, $\xi_4 = \log(4 + t^{-2}) \pm \log(\frac{\sqrt{4t^2+1}-1}{\sqrt{4t^2+1}+1})$ and $\xi_2 = \xi_3 = \log(4 + t^{-2})$ [see Fig. 2(a)]. The structure of the ES is different from that of usual Haldane-gap systems characterized by twofold degeneracy in all ES ($\xi_1 = \xi_4$ and $\xi_2 = \xi_3$) [22]. This is because our "Haldane" state is rather close to a Néel state which does not have edge spins, due to the lacking of the symmetries. We also get the von Neumann entanglement entropy $S_A = \sum_i \xi_i e^{-\xi_i}$ which approaches log 4 for large $t$. The finite entanglement entropy is a generic property of 1D gapped states [24].

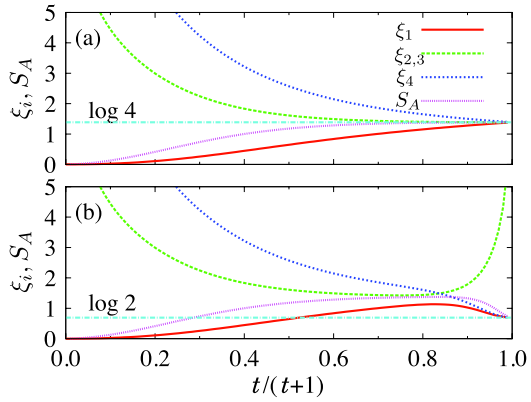


FIG. 2 (color online). Entanglement spectra $\{\xi_i\}$, and entanglement entropy $S_A$, as functions of $t$ for (a) infinite-size system and (b) finite-size ($N = 2L = 32$) system.

In finite systems, the entanglement properties are somewhat altered as shown in Fig. 2(b). Once the correlation length $\xi$ is of the order of the distance between the cuts $L$, the above structure of the ES breaks down [25] and for large enough $t$ the entanglement entropy is instead approaching log 2 due to the states $|+-+-\cdots\rangle$ and $|-+-+\cdots\rangle$.

*Compressibility and excitation gaps.*—When we shrink the system size as $N_s \to N_s - 1$ by removing 0 from the root state, a 10-type domain wall appears that carries a fractional charge [2] $e^* = e/3$ (The fractional charge follows from noting that creating three such domain walls 101010 amounts to adding one electron to the root state 100100). This excitation energy $E(N_s - 1)$ can be analytically calculated within a variational approach based on the MP formalism. Considering a subspace given by (6) where $|\Psi_0\rangle$ is replaced by $|\Psi^{-}_0\rangle = |10010100100\cdots\rangle$, and appropriate local deformation of the MP state, we get a finite value of $E(N_s - 1)$ for $N_s \to \infty$ as shown in Fig. 3. Since $E(N_s + 1) = E(N_s) = 0$ as already discussed, we obtain divergence of the inverse compressibility as expected for the FQH state,

$$\kappa^{-1} = \lim_{N_s\to\infty} N_s \frac{E(N_s - 1) + E(N_s + 1) - 2E_s(N_s)}{4\pi l_B^2} \to \infty. \quad (13)$$

The excitation energies in the charge neutral sector can also be calculated similarly. We specify these states by $\Delta K$ which means the center-of-mass coordinate relative to the ground state. Considering $\Delta K = 1$ and $\Delta K = 2$ subspaces given by (6), where $|\Psi_0\rangle$ is replaced by states $|\Psi_1\rangle = |100100010100\cdots\rangle$ and $|\Psi_2\rangle = |100010010100\cdots\rangle$, we get excellent agreement with the numerical results of the exact diagonalization which are very insensitive to the system size, as shown in Fig. 3. For $t = 1/3$, the $\Delta K = 1$ state is the lowest excitation only in the very small $\beta$ region, while the $\Delta K = 2$ state becomes the lowest as $\beta$ is increased. The tiny deviation at $\beta = 0$ is due to phase

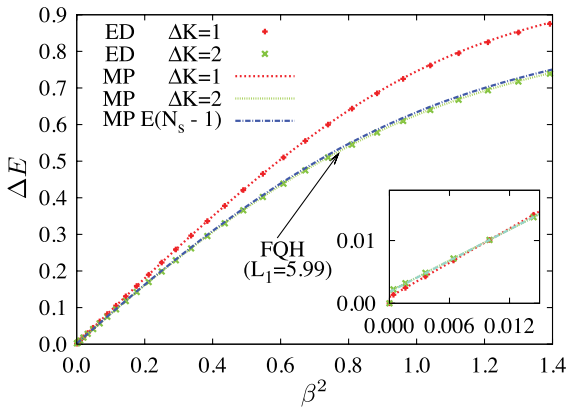


FIG. 3 (color online). The lowest excitation gaps of the model (3) at $\alpha = 1$, $t = 1/3$. The neutral gaps for $\Delta K = 1$, 2 are obtained by exact diagonalization (ED) for $N_s = 27$ (dots) and the variational calculation with the MP ansatz for $N_s \to \infty$ (lines). $E(N_s - 1)$ for $N_s \to \infty$ is also obtained by the MP ansatz. Here, $\beta^2 = 0.77$ corresponds to a FQH system on a torus with circumference $L_1 = 5.99$.

separated states, $|1010\cdots0000\rangle$, which have zero energy in this limit. The lowest $\Delta K = 0$ excitation is significantly higher in energy. Since the above features are qualitatively unchanged from small to sufficiently large $t$ regions ($|t| \sim 1$), we identify the $\Delta K = 2$ excitation gap as the neutral energy gap of a $\nu = 1/3$ FQH state with toroidal boundary conditions. This result is consistent with a recent analysis using the spherical geometry and the Jack polynomials which identifies the neutral gap in the $L = 2$ angular momentum sector [26].

*Bosonic systems.*—The present exact argument can also be applied to bosonic systems. The Hamiltonian (4) with the operators $Q_i = \alpha_i b_i b_i + \gamma_i b_{i-1} b_{i+1}$ and $P_i = \beta_i b_i b_{i+1}$ defines a $\nu = 1/2$ bosonic FQH state that has the following exact twofold degenerate ground state:

$$|\Psi^B_{1/2}\rangle = \prod_i \left(1 - \frac{t_i}{\sqrt{2}} b^\dagger_{i+1} b^\dagger_{i+1} b_{i+2} b_i\right) |\Psi^B_0\rangle, \qquad (14)$$

where $|\Psi^B_0\rangle \equiv |0101010\cdots\rangle$ and $t_i \equiv \gamma_i/\alpha_i$. In this model the spin-1 mapping is also possible as $|10\rangle \to |o\rangle$, $|02\rangle \to |+\rangle$, and $|00\rangle \to |-\rangle$. Hence, we obtain the same effective spin-1 representation (7) as in the $\nu = 1/3$ fermion system.

*Conclusion.*—We have introduced a 1D interacting fermion model with an exact ground state that describes a $\nu = 1/3$ FQH state. We have demonstrated the uniqueness of the ground state with periodic boundary conditions for each center-of-mass sector. We have introduced a MP representation of the ground states and obtained exact expressions for various correlation functions, order parameters, and the entanglement spectra. Moreover, the excitation gaps have been accurately obtained via variational calculations with MP ansatz. We have also shown that the present argument can be applied to a $\nu = 1/2$ bosonic FQH state. Although our thin-torus approach does not describe a genuine liquid state [11], it captures other important aspects of the FQH physics.

We thank Juha Suorsa for useful discussions and for related collaborations. M. N. and E. J. B. acknowledge the visitors program of the Max Planck Institute für Physik komplexer Systeme, Dresden, where this work was initiated. M. N. acknowledges support from Global Center of Excellence Program "Nanoscience and Quantum Physics" of the Tokyo Institute of Technology and Grants-in-Aid No. 23540362 by MEXT. E. J. B. was supported by the Alexander von Humboldt Foundation.

[1] D. C. Tsui, H. L. Stormer, and A. C. Gossard, Phys. Rev. Lett. **48**, 1559 (1982).
[2] R. B. Laughlin, Phys. Rev. Lett. **50**, 1395 (1983).
[3] See, e.g., E. Tang, J.-W. Mei, and X.-G. Wen, Phys. Rev. Lett. **106**, 236802 (2011); T. Neupert, L. Santos, C. Chamon, and C. Mudry, *ibid.* **106**, 236804 (2011); K. Sun, Z. Gu, H. Katsura, and S. Das Sarma, *ibid.* **106**, 236803 (2011).
[4] Y.-J. Lin, R. L. Compton, K. Jiménez-García, J. V. Porto, and I. B. Spielman, Nature (London) **462**, 628 (2009).
[5] E. J. Bergholtz and A. Karlhede, Phys. Rev. Lett. **94**, 026802 (2005).
[6] A. Seidel, H. Fu, D.-H. Lee, J. M. Leinaas, and J. Moore, Phys. Rev. Lett. **95**, 266405 (2005).
[7] X.-L. Qi, Phys. Rev. Lett. **107**, 126803 (2011).
[8] I. Affleck, T. Kennedy, E. H. Lieb, and H. Tasaki, Phys. Rev. Lett. **59**, 799 (1987); Commun. Math. Phys. **115**, 477 (1988).
[9] S. A. Trugman and S. A. Kivelson, Phys. Rev. B **31**, 5280 (1985).
[10] E. J. Bergholtz and A. Karlhede, J. Stat. Mech. 2006, L04001; Phys. Rev. B **77**, 155308 (2008).
[11] E. H. Rezayi and F. D. M. Haldane, Phys. Rev. B **50**, 17199 (1994).
[12] H. Wang and V. W. Scarola, Phys. Rev. B **83**, 245109 (2011).
[13] We find that the overlap integral of the wave functions of the full (1) and the truncated (3) Hamiltonians calculated by exact diagonalization is over 0.98 up to $L_1 \approx 7$ for $N_s = 18$.
[14] S. Jansen, arXiv:1109.4022.
[15] Z.-Y. Wang, S. Takayoshi, and M. Nakamura, arXiv:1205.4850.
[16] M. Fannes, B. Nachtergale, and R. F. Werner, Europhys. Lett. **10**, 633 (1989); Commun. Math. Phys. **144**, 443 (1992).
[17] A. Klümper, A. Schadschneider, and J. Zittartz, Z. Phys. B **87**, 281 (1992); Europhys. Lett. **24**, 293 (1993).
[18] M. Nakamura, E. J. Bergholtz, and J. Suorsa, Phys. Rev. B **81**, 165102 (2010); E. J. Bergholtz, M. Nakamura, and J. Suorsa, Physica E (Amsterdam) **43**, 755 (2011).
[19] This corresponds to $L_1 \sim 10.25$, which is beyond the region where Eq. (6) quantitatively describes the FQH state.
[20] M. den Nijs and K. Rommelse, Phys. Rev. B **40**, 4709 (1989).

[21] E. Berg, E. G. Dalla Torre, T. Giamarchi, and E. Altman, Phys. Rev. B **77**, 245119 (2008).
[22] F. Pollmann, A. M. Turner, E. Berg, and M. Oshikawa, Phys. Rev. B **81**, 064439 (2010).
[23] H. Li and F. D. M. Haldane, Phys. Rev. Lett. **101**, 010504 (2008).
[24] J. Eisert, M. Cramer, and M. B. Plenio, Rev. Mod. Phys. **82**, 277 (2010).
[25] A. M. Läuchli, E. J. Bergholtz, J. Suorsa, and M. Haque, Phys. Rev. Lett. **104**, 156404 (2010).
[26] B. Yang, Z.-X. Hu, Z. Papic, and F. D. M. Haldane, Phys. Rev. Lett. **108**, 256807 (2012).